

Ignition-promoting effect of NO₂ on methane, ethane and methane/ethane mixtures in a rapid compression machine

S. Gersen^a, A.V. Mokhov^b, J.H. Darmeveil^a, H.B. Levinsky^{a,b,*},
P. Glarborg^c

^a KEMA Nederland B.V., P.O. Box 2029, 9704 CA Groningen, The Netherlands

^b Laboratory for High Temperature Energy Conversion Processes, University of Groningen, Nijenborgh 4, 9747 AG Groningen, The Netherlands

^c DTU Chemical Engineering, Technical University of Denmark, DK-2800 Kgs. Lyngby, Denmark

Available online 23 August 2010

Abstract

Autoignition delay times of stoichiometric methane, ethane and methane/ethane mixtures doped with 100 and 270 ppm of NO₂ have been measured in a RCM in the temperature range 900–1050 K and pressures from 25 to 50 bar. The measurements show that addition of NO₂ to CH₄/O₂/N₂/Ar and CH₄/C₂H₆/O₂/N₂/Ar mixtures results in a significant reduction in the autoignition delay time and that the ignition-promoting effect of NO₂ increases substantially with increasing temperature, from ~20% to more than a factor of two over the range of temperature studied. Addition of NO₂ to C₂H₆/O₂/N₂/Ar mixtures results in only a modest reduction in ignition delay time over the range of pressure and temperature measured. Computations with an updated chemical mechanism show good agreement with the measurements for undoped methane, but overpredict the delay times for undoped ethane and underestimate the effects of replacing 10% methane by ethane. For NO₂-containing mixtures, the model predicts the observed trend in decreasing delay time with increasing NO₂ fraction. However, the computations tend to overestimate the effect of NO₂ addition on ignition, particularly for C₂H₆ mixtures. Analysis of the reaction mechanism for the effects of NO₂ addition to methane mixtures indicates that the ignition-promoting effect of NO₂ is related to the appearance of new conversion channels for CH₃ and CH₃OO, i.e., NO₂ + CH₃ → NO + CH₃O and NO + CH₃OO → NO₂ + CH₃O, generation of chain-initiating OH radicals through NO/NO₂ interconversion, i.e., NO₂ + H → NO + OH and NO + HO₂ → NO₂ + OH, and to the direct initiation step CH₄ + NO₂ → CH₃ + HNO₂. Analyses further show that the formation of CH₃NO₂ via CH₃ + NO₂(+M) ↔ CH₃NO₂(+M) essentially inactivates NO₂. This reaction limits the promoting effect of NO₂ at lower temperatures and higher pressures, where stabilization of CH₃NO₂ is favored, explaining the experimentally observed trends.

© 2010 The Combustion Institute. Published by Elsevier Inc. All rights reserved.

Keywords: Autoignition; NO_x sensitization; Alkane oxidation; Rapid compression machine

* Corresponding author at: KEMA Nederland B.V., P.O. Box 2029, 9704 CA Groningen, The Netherlands. Fax: +31 50 7009858.

E-mail address: howard.levinsky@kema.com (H.B. Levinsky).

1. Introduction

The impact of small amounts of NO_x on the oxidation characteristics of fuels at high pressure and moderate temperatures is important in practical combustion equipment. For example, in HCCI engines exhaust gas recirculation (EGR) is used to lower combustion temperatures as a NO_x -control strategy. However, a side effect of EGR is the reduction of the ignition delay time arising from the presence of NO_x in the recirculated exhaust gas [1]. Since the operation of HCCI engines is controlled by the autoignition behavior of the fuel, detailed knowledge of the effects of NO_x on the ignition delay times of fuels is necessary for design and operation of these engines. Inasmuch as the performance of stationary spark-ignited (natural gas) engines used for power generation and automotive engines using compressed natural gas (CNG) is often limited by engine knock, any promotion of autoignition by NO_x is important when considering mixing exhaust gases with the fuel–air mixture, either deliberately for NO_x control or unintentionally during intake and compression. As such, insight into the effects of NO_x on autoignition is important for these developments.

The interaction of NO_x chemistry with fuel oxidation has been studied for several fuels, such as methane/natural gas [2–15] and C_2 hydrocarbons [3,5,16–19], most of them performed at pressures lower than ~ 10 bar. Using experiments and modeling, mainly in flow reactors and jet-stirred reactors, these kinetic studies showed that NO_x addition promotes oxidation of the fuels and that hydrocarbons promote the conversion of NO to NO_2 . Recently, the oxidation-enhancing effect of NO_x on dilute methane–ethane mixtures has been studied at high pressure (~ 50 bar) and temperatures ranging from ~ 1070 to 1500 K by sampling and measuring the major oxidation products as a function of temperature in a shock tube [14]. The study showed that the oxidation of the natural gas blend was enhanced even when small amounts of NO were present. The sensitizing effect of NO_x on CH_4 oxidation at 20, 50 and 100 bar at 600–900 K was also recently investigated in a high pressure laminar flow reactor [15], where the reactants were highly diluted to minimize heat release during

reaction. The results demonstrated a significant decrease in the initiation temperature of reaction upon addition of NO_x , and a similar effect was observed with increasing pressure. The authors further showed that the sensitizing effect of NO_x is due to the hydrocarbon chain-propagating reactions $\text{NO}_2 + \text{CH}_3 \leftrightarrow \text{NO} + \text{CH}_3\text{O}$ and $\text{NO} + \text{CH}_3\text{OO} \leftrightarrow \text{NO}_2 + \text{CH}_3\text{O}$. Previous work in a flow reactor [9] indicated that NO and NO_2 have a similar impact on the onset of reaction of CH_4 . Although it is known that the oxidation of fuels is accelerated by the addition of NO_x , the actual effect on ignition phenomena has only been studied for undiluted hydrogen–air mixtures, by measuring autoignition delay times in shock tubes at conditions ranging from 800 to 1500 K and pressures below 4 bar [20,21]. To our knowledge, no measurements have been performed to study the effects of NO_x addition on the autoignition delay times of hydrocarbon fuels under conditions relevant to spark-ignited and HCCI engines.

In this paper, we study the effects of the addition of small fractions of NO_2 to stoichiometric $\text{CH}_4/\text{O}_2/\text{N}_2/\text{Ar}$, $\text{C}_2\text{H}_6/\text{O}_2/\text{N}_2/\text{Ar}$ and $\text{CH}_4/\text{C}_2\text{H}_6/\text{O}_2/\text{N}_2/\text{Ar}$ mixtures on autoignition, by measuring ignition delay times in a RCM at pressures from 25 to 50 bar and temperatures in the range 900–1050 K. The measurements performed in this study are discussed in the context of numerical calculations performed using an update of a recently developed mechanism [15].

2. Experimental procedure

The experimental set-up and the procedure for the ignition measurements performed in the rapid compression machine are described in detail elsewhere [22,23], and here we highlight the specific aspects of the experiments under consideration. Methane, ethane and a methane/ethane mixture (in a ratio of 90:10) were combined with $\text{O}_2/\text{N}_2/\text{Ar}$ oxidizer to stoichiometric proportions and doped with either 100 or 270 ppm of NO_2 . Table 1 gives the compositions of the fuel–oxidizer mixtures studied, expressed in mole percent. The mixtures were manometrically prepared in advance in a 10L gas cylinder and allowed to

Table 1
Composition of mixtures, mole percentages.

Mixture	CH_4 (%)	C_2H_6 (%)	NO_2 (%)	O_2 (%)	N_2 (%)	Ar (%)
A	9.09	0	0	18.18	30.00	42.73
B	9.08	0	0.01	18.18	30.00	42.73
C	9.07	0	0.027	18.18	30.00	42.73
D	0	5.40	0	18.92	30.00	45.68
E	0	5.40	0.01	18.92	30.00	45.67
F	0	5.39	0.027	18.92	30.00	45.66
G	7.66	0.85	0	18.30	30.00	43.19
H	7.64	0.85	0.027	18.30	30.00	43.19

mix for ~ 72 h. We note that dopant was originally added as NO, using 900 ± 9 ppm NO in N_2 , which was completely converted to NO_2 via $NO + NO + O_2 \leftrightarrow 2NO_2$ [15]. Total conversion was verified by a UV absorbance analyzer (ABB model LIMAS 11 UV); this measurement also indicated that the NO_2 fraction in the mixtures as reported here were within 1% of the target value. All pure gases used in the experiments have purity greater than 99.99%. The ratio of total inert gases (Ar, N_2) to oxygen in our mixtures is close to the ratio of nitrogen to oxygen in air. The proportions of diluent gases (Ar, N_2) were chosen to achieve the desired peak gas temperatures after compression, T_c , over the range of ~ 900 – 1050 K, at peak pressures after compression, P_c , from 25 to 50 bar for the methane/ NO_2 /oxidizer and methane/ethane/ NO_2 /oxidizer mixtures, while temperatures from ~ 930 to 1010 K and pressures from 20 to 40 bar were studied for the ethane/ NO_2 /oxidizer mixtures.

To avoid the difficulty of calculating an effective compression ratio based on the uncertain actual physical volume in the combustion chamber, the temperature after compression T_c is determined by numerically solving the following equation [23],

$$\ln \frac{P_c}{P_i} = \int_{T_i}^{T_c} \frac{\gamma}{\gamma - 1} d \ln T \quad (1)$$

using the thermodynamic data of Rasmussen et al. [15] together with the measured pre-ignition peak pressure P_c , and the measured initial pressure P_i and temperature T_i of the mixture. In general the “day-to-day” reproducibility of the measured ignition delay times performed under identical conditions is $\sim 5\%$. The positioning reproducibility of the compression ratio yielded a variation in T_c of ± 2 K, which gave a slightly larger variation in experimental results in measurements taken along an isotherm.

3. Simulation procedure

The experimental results have been analysed in terms of a detailed chemical kinetic model for the oxidation of C_1 and C_2 hydrocarbons, both with and without NO_2 . The starting mechanism and the corresponding thermodynamic properties were drawn from the high-pressure work by Rasmussen and co-workers on conversion of CO/H_2 and C_1/C_2 hydrocarbons, with and without NO_x [15,24–27]. A few changes were made in the present work. A number of reactions between hydrocarbon and peroxide species was included, taken from the mechanism of Petersen et al. [28]. For the reactions between CH_4 and NO_2 to yield CH_3 and $HONO/HNO_2$, we take the rate constants from the evaluation of Dean and Bozzelli [29] for the reverse steps. Their estimates are consistent with the only

experimental determination, a shock tube study by Slack and Grillo [30]. For the reactions of C_2H_6 and C_2H_4 with NO_2 , we find that the rough estimates of Rasmussen et al. [15] lead to too high values of the reverse rate constants of HNO_2 with C_2H_5 and C_2H_3 , respectively. Instead we assume the C_2H_5/C_2H_3 reactions with $HONO$ and HNO_2 to have rate coefficients similar to the corresponding steps of CH_3 . The full mechanism is available as [Supplementary data](#).

During the rapid compression machine experiments deviations from ideal behavior, such as heat loss, occur. Previous research [22,23,31–35] has shown the importance of accounting for these deviations from ideal behavior when simulating RCM ignition experiments. For this purpose the specific volume of the assumed adiabatic core is often used as input in the simulations. As was done in our recent study [23], one method to do this is to calculate the specific volume from the pressure trace measured in an inert mixture having the same heat capacity, initial pressure and initial temperature as that of the reactive mixture under investigation, and by using the adiabatic relations between pressure, volume and temperature. Since no multistage ignition phenomena were observed in this study, we used a simpler method described previously [22]. In this method, the specific volume is derived directly by (exponentially) fitting the measured pressure trace for the reactive mixture in the period between compression and the time after compression at which substantial heat release begins (~ 1 ms prior the minimum in the pressure trace); after this point the pressure is extrapolated using the fit [22]. The specific volume thus derived is used as input into the simulations, which used the SENKIN code [36]. The results of the method are illustrated in Fig. 1, which shows the experimental pressure trace for mixture A in Table 1 and the pressure trace based on the fitting-and-extrapolation method described above that is used to obtain the specific volume for the simulations. In addition, the results of two simulations are shown: the pressure profile computed by using the specific volume trace by the method just described and the profile derived from the measured pressure trace using an inert mixture. Since the two simulated profiles are nearly indistinguishable, for the results presented here we derive the specific volume from the reactive mixture, rather than from the more labor-intensive inert mixtures. Figure 1 also shows that the simulated pressure profile obtained with the mechanism used [15] is in qualitative agreement with the experiment, and the simulated ignition delay time is within $\sim 10\%$ of that measured. For ignition delay times shorter than 3 ms the experimental pressure traces show in general no pressure decay. For these conditions, the volume after compression was kept constant in the simulations. Although not shown, for these short times

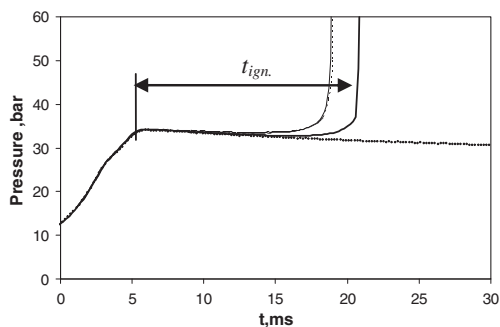


Fig. 1. Measured and modeled pressure traces for mixture A at $T_c \sim 972$ K. Bold solid line: measured pressure trace. Bold dotted line: pressure trace derived from specific volume using fit-and-extrapolated measured trace, as described in the text. Thin solid line: simulated pressure trace using extrapolated specific volume. Thin dashed line: modeled pressure trace using the specific volume derived from measured pressure trace in inert mixture. Calculations performed using the detailed mechanism.

the agreement between the simulated traces using the method described here and those obtained from experiments using inert mixtures was as good as that shown in Fig. 1 for longer ignition delay times. We also remark that the pressure trace during compression for short delay times was identical to those of the equivalent inert mixture, ensuring that there was no heat release during compression.

4. Results and discussion

4.1. Experimental results

Figure 2 presents the temperature dependence of the measured ignition delay time for pure methane (mixture A) and methane/ NO_2 (mixtures B and C) at a pressure after compression (P_c) of ~ 40 bar. This figure illustrates the significant ignition-enhancing effect of NO_2 addition to methane, and that this effect is temperature dependent. At high temperatures the ignition-promoting effect of NO_2 addition is more pronounced than at low temperatures. For example, at $T_c \sim 1010$ K addition of 270 ppm NO_2 (mixture C) to the methane/oxidizer mixture results in a reduction in the autoignition delay time of more than a factor of two, while at $T_c \sim 910$ K the reduction in ignition delay is only $\sim 20\%$. It is interesting to note that in contrast to this observation the ignition-promoting effect of NO_2 addition to hydrogen, measured at 2 bar in a shock tube [20], decreases with increasing temperature. The measurements performed along the isotherm at $T_c = 995 \pm 2$ K, shown in Fig. 3, illustrate the effect of NO_2 on ignition for P_c between 25 and

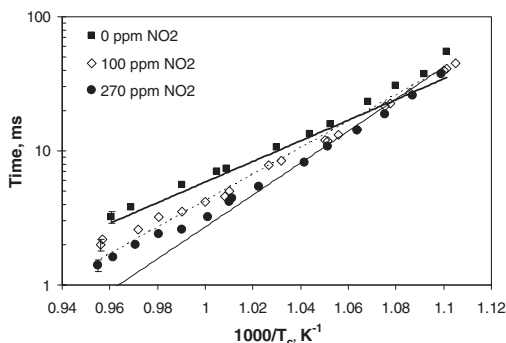


Fig. 2. Effect of NO_2 addition on autoignition delay time of methane mixtures as function of temperature at $P_c \sim 40 \pm 0.5$ bar. Measured (symbols) and predicted (lines) delay times in mixtures A (no added NO_2 , squares, bold solid line), B (100 ppm NO_2 , diamonds, dashed line) and C (270 ppm NO_2 , circles, thin solid line).

50 bar. Reminiscent of previous flow reactor experiments at high pressure [15], showing a decrease in initiation temperature with increasing pressure for methane/ NO_x mixtures, the ignition delay time of methane/ NO_2 mixtures decreases substantially with increasing pressure. Further, the results suggest that the decrease in ignition delay time as function of the NO_2 fraction added is larger at lower pressure. We shall discuss the observed behavior further below, in the context of the analysis of the chemical mechanism. We note that the plots of the logarithm of the ignition delay times versus the reciprocal temperature (Figs. 2, 4 and 6, see below) suggest an Arrhenius-type relation for all mixtures, at least in the limited region of temperature studied here. Since the measured ignition delay times depend

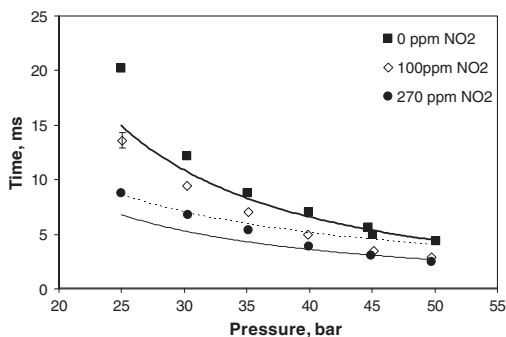


Fig. 3. Effect of NO_2 addition on autoignition delay time of methane mixtures as function of pressure at $T_c \sim 995 \pm 2$ K. Measured (symbols) and predicted (lines) delay times in mixtures A (no added NO_2 , squares, bold solid line), B (100 ppm NO_2 , diamonds, dashed line) and C (270 ppm NO_2 , circles, thin solid line).

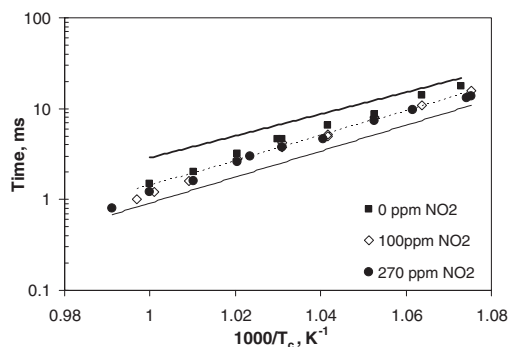


Fig. 4. Effect of NO_2 addition on autoignition delay time of ethane mixtures as function of temperature at $P_c \sim 30 \pm 0.5$ bar. Measured (symbols) and predicted (lines) delay times in mixtures D (no added NO_2 , squares, bold solid line), E (100 ppm NO_2 , diamonds, dashed line) and F (270 ppm NO_2 , circles, thin solid line).

significantly upon the heat losses in the pre-ignition period, with longer delay times showing more heat loss, we refrain from extracting effective activation energies from these data.

Significantly different behavior is seen in the ethane mixtures (mixtures D, E and F), illustrated in Fig. 4. At $P_c \sim 30$ bar, we see that the addition of NO_2 to ethane results in only a modest reduction in the autoignition delay time, and with no clear temperature dependence of the ignition-enhancing effect of NO_2 over the, albeit limited, range of temperature studied. The generally modest effect is also observed in the isotherms at $T_c = 960 \pm 2$ K, presented in Fig. 5, which also shows a decrease in ignition delay time with increasing pressure, similar to that seen for meth-

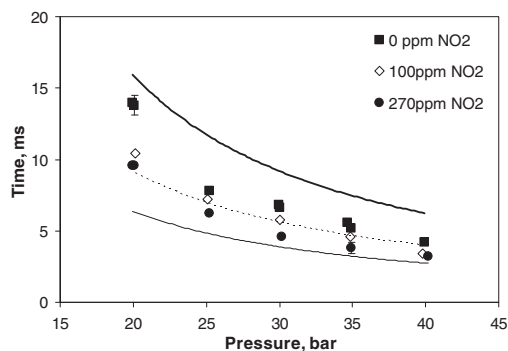


Fig. 5. Effect of NO_2 addition on autoignition delay time of ethane mixtures as function of pressure at $T_c \sim 960 \pm 2$ K. Measured (symbols) and predicted (lines) delay times in mixtures D (no added NO_2 , squares, bold solid line), E (100 ppm NO_2 , diamonds, dashed line) and F (270 ppm NO_2 , circles, thin solid line).

ane in Fig. 2. Overall, the addition of 270 ppm NO_2 results in a reduction in the autoignition delay time of about 20–30% over the range of pressures and temperatures studied, similar in magnitude to the effect seen in Fig. 2 for methane at T_c lower than ~ 950 K.

In addition to pure methane and ethane fuels, the effects of NO_2 addition on the ignition properties of $\text{CH}_4\text{--C}_2\text{H}_6$ mixtures have been studied. The methane/ethane ratio is 90:10 (mixtures G and H), not uncommon for realistic natural gases. Figure 6, giving the temperature dependence of ignition at $P_c \sim 40$ bar, clearly shows that replacing 10% methane by ethane (mixture G) substantially reduces the ignition delay time, and that this reduction is also dependent upon temperature. At $T_c \sim 900$ K, ethane reduces the delay time by roughly 50%, while at ~ 1040 K this reduction is a factor of two. The ignition-promoting effect of ethane addition to methane was also observed previously in shock tube measurements [37], under similar conditions to those reported here. As can be seen in Fig. 6, the addition of 270 ppm NO_2 in the $\text{CH}_4/\text{C}_2\text{H}_6/\text{O}_2/\text{N}_2/\text{Ar}$ mixture significantly reduces the ignition delay time further. This is similar to the behavior reported in [6], in which small fractions of NO_2 were seen to reduce the initial reaction temperature significantly of both methane and methane/ethane mixtures in a flow reactor at temperatures ranging from 800 to 975 K and $P \sim 10$ bar. We further note that the NO_2 -induced reduction in ignition delay time for the methane/ethane mixture is also temperature dependent: comparing the data for mixtures G and H in Fig. 6 shows that the additional reduction caused by NO_2 is nearly a factor of two at $T_c \sim 1040$ K, but by less than 30% at ~ 900 K. We also observe that the slope of the plots is increased upon adding both ethane (mixture G) and by ethane/ NO_2

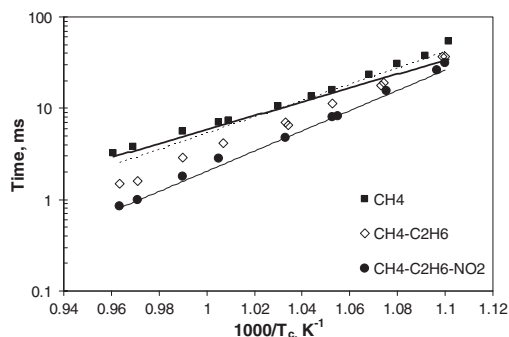


Fig. 6. Effects of ethane and NO_2 addition on autoignition delay time of methane mixtures as a function of temperature at $P_c \sim 40 \pm 0.5$ bar. Measured (symbols) and predicted (lines) delay times in mixtures A (methane fuel, squares, bold solid line), G (fuel 90% methane/10% ethane, diamonds, dashed line) and H (methane/ethane mixture with 270 ppm NO_2 , circles, thin solid line).

(mixture H) as compared to pure methane (mixture A).

4.2. Simulation results

The experimental results have been analysed in terms of a detailed chemical kinetic model for the oxidation of C₁ and C₂ hydrocarbons, both with and without NO₂. The predictions for pure methane mixtures (mixture A) in Figs. 2 and 3 are all within 20% of the measurements. For the methane/NO₂ mixtures (mixtures B and C) the computations capture the qualitative trends well, but tend to underpredict slightly the ignition delay above 1000 K (Fig. 2) and at lower pressures (Fig. 3).

Reaction path analysis and sensitivity analysis of the modeling results show that the ignition delay is mainly governed by the fate of the relatively unreactive methyl and methyl peroxide radicals. For pure methane, the CH₃ radical is converted to CH₂O, either directly by reaction with O₂ or through formation of methyl peroxide and methoxy, $\text{CH}_3 \xrightarrow{+\text{O}_2} \text{CH}_3\text{OO} \xrightarrow{+\text{CH}_3} \text{CH}_3\text{O} \xrightarrow{+\text{M}, \text{O}_2} \text{CH}_2\text{O}$. In addition to CH₃OO, the high pressure favors formation of HO₂, and the predicted ignition delay is sensitive to its reaction with CH₄, as well as to the products of the CH₃ + HO₂ reaction, which may be chain propagating (CH₃O + OH) or chain terminating (CH₄ + O₂).

The addition of NO₂ to the mixture opens up new conversion channels for CH₃ and CH₃OO, i.e., $\text{NO}_2 + \text{CH}_3 \rightarrow \text{NO} + \text{CH}_3\text{O}$ and $\text{NO} + \text{CH}_3\text{OO} \rightarrow \text{NO}_2 + \text{CH}_3\text{O}$. These steps facilitate chain branching and serve to explain the sensitization of CH₄ by NO_x, as observed in previous studies [4,9–12,14,15,38,39]. Moreover, the promoting effect of NO₂ is related to NO/NO₂ interconversion ($\text{NO}_2 + \text{H} \rightarrow \text{NO} + \text{OH}$; $\text{NO} + \text{HO}_2 \rightarrow \text{NO}_2 + \text{OH}$) that serves to generate chain-initiating OH radicals, and to the direct initiation step $\text{CH}_4 + \text{NO}_2 \rightarrow \text{CH}_3 + \text{HNO}_2$. Due to the interconversion between NO and NO₂, modeling predictions indicate that the ignition delays are not sensitive to the partitioning of NO_x between NO and NO₂. This is in agreement with observation from flow reactor experiments [9].

Our analysis shows that the recombination reaction $\text{CH}_3 + \text{NO}_2(+\text{M}) \leftrightarrow \text{CH}_3\text{NO}_2(+\text{M})$ retards the ignition process under the present conditions, essentially by temporarily removing reactive NO₂ from the mixture. Substantial formation of CH₃NO₂ was observed at high pressure for the CH₄/O₂/NO_x system by Rasmussen et al. [15], but has to our knowledge not been reported at atmospheric pressure. The recombination reaction is responsible for the formation of CH₃NO₂, while the reverse step, thermal dissociation, is the main consumption channel for nitromethane. The computations indicate that CH₃NO₂ remains stable until fuel and oxidizer approach depletion. In this

way, the formation of CH₃NO₂ causes a temporary inactivation of NO₂ in the initial phase of the ignition process at high pressure, which slows the overall oxidation of the hydrocarbon.

The competition between the two product channels for CH₃ + NO₂, which is important for the sensitizing effect of NO₂, depends on temperature and pressure. An increase in pressure and a decrease in temperature both favor stabilization of CH₃NO₂, i.e., chain termination. For this reason, the promoting effect of NO_x should become more pronounced at higher temperatures and lower pressures; this trend is confirmed by the results of Figs. 2 and 3. The differences between the observed and predicted pressure and temperature dependence may conceivably be attributed to uncertainties regarding the formation and stability of nitromethane. Furthermore, at the lower end of the present temperature range, the assumption that the rate constant for $\text{NO}_2 + \text{CH}_3 \rightarrow \text{NO} + \text{CH}_3\text{O}$ is independent of pressure may not be valid; more work is desirable to clarify this point.

The modeling predictions for pure ethane mixtures (mixture D), seen in Figs. 4 and 5, show a substantial overprediction, up to a factor of two, of the ignition delay. The reason for this discrepancy is not clear, but may be due to deficiencies regarding the rate constants for C₂H₆ with O₂ and HO₂, which are both uncertain, or in the C₂H₅OO/C₂H₅OOH subset of the mechanism. The mechanism of Petersen et al. [28], which also includes a C₃ subset but contains no reactions involving NO_x, provides a good prediction of the ignition delays for both CH₄ and C₂H₆, mixtures A and D (data not shown).

The trends for the ethane/NO₂ mixtures (mixtures E and F) as compared to pure ethane, seen in Figs. 4 and 5, are well reproduced, with perhaps coincidentally good agreement for mixture E (100 ppm NO₂). The computations for mixture F (270 ppm NO₂) tend to predict larger reductions in the ignition delay time as compared to the measurements for nearly all conditions studied. From Fig. 6 it is clear that, in contradiction with the measurements, the computations predict only modest effect on the calculated ignition delay time upon replacement of 10% methane by ethane, while the addition of NO₂ to the mixture (mixture H) is overestimated.

Despite the quantitative differences, the model predictions are in agreement with the observed trends, and analysis of the calculations offers some insight into the mechanism of sensitization. According to the model, the promoting effect of NO₂ on C₂H₆ ignition can be attributed to a set of reactions similar to that governing the CH₄/NO_x interactions. The presence of NO₂ promotes ignition through the direct initiation step $\text{C}_2\text{H}_6 + \text{NO}_2 \rightarrow \text{C}_2\text{H}_5 + \text{HNO}_2$. Chain branching is enhanced through the reaction $\text{C}_2\text{H}_5 + \text{NO}_2 \rightarrow$

$\text{C}_2\text{H}_5\text{O} + \text{NO}$ which competes with $\text{C}_2\text{H}_5 + \text{O}_2 \rightarrow \text{C}_2\text{H}_4 + \text{HO}_2$. Also, reactions of peroxides with NO , i.e., $\text{NO} + \text{HO}_2 \rightarrow \text{NO}_2 + \text{OH}$ and $\text{C}_2\text{H}_5\text{OO} + \text{NO} \rightarrow \text{C}_2\text{H}_5\text{O} + \text{NO}_2$, serve to promote oxidation, while the recombination reaction $\text{C}_2\text{H}_5 + \text{NO}_2(+\text{M}) \rightarrow \text{C}_2\text{H}_5\text{NO}_2(+\text{M})$ delays ignition.

The major uncertainties in this subset concern the reactions of C_2H_6 and C_2H_5 with NO_2 . The rate constant for the initiation step of $\text{C}_2\text{H}_6 + \text{NO}_2$ is only a rough estimate, based on an analogy between reactions of C_2H_5 and CH_3 with HONO and HNO_2 . The rate coefficients for the disproportionation channel $\text{C}_2\text{H}_5 + \text{NO}_2 \rightarrow \text{C}_2\text{H}_5\text{O} + \text{NO}$ were also assumed to be similar to those of $\text{CH}_3 + \text{NO}_2$. For the recombination channel, data have been reported for the reverse step [40], and the thermal decomposition of $\text{C}_2\text{H}_5\text{NO}_2$ to C_2H_5 and NO_2 was studied in a shock tube at 900–1350 K and 0.33–33 bar, where the reaction is near the high-pressure limit. In order to reconcile these results with data [41–44] obtained at lower temperatures and pressures (593–715 K, 0.1–1 bar), the high-pressure limiting rate coefficient was modified in [15], while retaining the low-pressure limit from [44]. However, the resulting estimates for the two product channels of $\text{C}_2\text{H}_5 + \text{NO}_2$ are not consistent with the room-temperature value of the branching ratio reported by others [45]. More work on this and other reactions is desirable to account better for the differences in NO_x -enhanced ignition between methane and ethane.

5. Conclusion

Autoignition delay times of stoichiometric methane, ethane and methane/ethane mixtures doped with small fractions NO_2 (100 and 270 ppm) have been measured in a RCM in the temperature range 900–1050 K and pressures from 25 to 50 bar. The measurements show that addition of NO_2 to $\text{CH}_4/\text{O}_2/\text{N}_2/\text{Ar}$ and $\text{CH}_4/\text{C}_2\text{H}_6/\text{O}_2/\text{N}_2/\text{Ar}$ mixtures results in significant reduction in the autoignition delay time and that the ignition-promoting effect of NO_2 increases substantially with temperature. Addition of NO_2 to $\text{C}_2\text{H}_6/\text{O}_2/\text{N}_2/\text{Ar}$ mixtures results in only a modest reduction in ignition delay time over the range of measured pressures and temperatures. The experimental results are compared to modeling predictions with a detailed chemical kinetic model. Good agreement is observed between calculated and measured ignition delay times for undoped methane mixtures. Computed delay times for methane/ NO_2 mixtures are generally shorter than those observed experimentally but predict the trends of well, although tending to overpredict the temperature dependence and underpredict the pressure dependence. Calculations for pure ethane

mixtures overpredict the ignition delay times compared to the measurements, and computed effect of the addition of NO_2 to the ethane is somewhat larger than that measured. In contrast to the measurements, the computations predict little effect of replacing 10% methane by ethane, while the reduction in delay time upon NO_2 addition to the methane/ethane mixture is overestimated. Analysis of the reaction mechanism indicates that the ignition-promoting effect of NO_2 on methane arises from the new conversion channels for CH_3 and CH_3OO , i.e., $\text{NO}_2 + \text{CH}_3 \rightarrow \text{NO} + \text{CH}_3\text{O}$ and $\text{NO} + \text{CH}_3\text{OO} \rightarrow \text{NO}_2 + \text{CH}_3\text{O}$. Moreover, the promoting effect of NO_2 is related to the NO/NO_2 interconversion that serves to generate chain-initiating OH radicals, and to the direct initiation step $\text{CH}_4 + \text{NO}_2 \rightarrow \text{CH}_3 + \text{HNO}_2$. Analyses further show that the formation of CH_3NO_2 via $\text{CH}_3 + \text{NO}_2(+\text{M}) \leftrightarrow \text{CH}_3\text{NO}_2(+\text{M})$ essentially inactivates NO_2 . That lower temperatures and higher pressures favor the stabilization of CH_3NO_2 explains the experimentally observed enhanced effect of NO_2 addition at higher temperatures.

Acknowledgement

We gratefully acknowledge support of the N.V. Nederlandse Gasunie for this work.

Appendix A. Supplementary data

Supplementary data associated with this article can be found, in the online version, at [doi:10.1016/j.proci.2010.05.097](https://doi.org/10.1016/j.proci.2010.05.097).

References

- [1] A. Dubreuil, F. Foucher, C. Mounaim-Rousselle, G. Dayma, P. Dagaut, *Proc. Combust. Inst.* 31 (2007) 2879–2886.
- [2] N. Murakami, J. Izumi, S. Shirakawa, *Nenryo Kyokai-shi* 61 (1982) 329–337.
- [3] M. Hori, N. Matsunaga, P.C. Malte, N.M. Marinov, *Proc. Combust. Inst.* 24 (1992) 909–916.
- [4] J.H. Bromly, F.J. Barnes, S. Muris, X. You, B.S. Haynes, *Combust. Sci. Tech.* 115 (1996) 259–296.
- [5] M. Hori, N. Matsunaga, N.M. Marinov, W. Pitz, C. Westbrook, *Proc. Combust. Inst.* 27 (1998) 389–396.
- [6] T. Amano, F.L. Dryer, *Proc. Combust. Inst.* 27 (1998) 397–404.
- [7] Y. Yamaguchi, Y. Teng, S. Shimomura, K. Tabata, E. Suzuki, *J. Phys. Chem. A* 103 (1999) 8272–8278.
- [8] K. Tabata, Y. Teng, Y. Yamaguchi, H. Sakurai, E. Suzuki, *J. Phys. Chem. A* 104 (2000) 2648–2654.
- [9] A.B. Bendtsen, P. Glarborg, K. Dam-Johansen, *Combust. Sci. Tech.* 151 (2000) 31–71.
- [10] A.A. Konnov, J.N. Zhu, J.H. Bromly, D.K. Zang, *Proc. Combust. Inst.* 30 (2005) 1093–1100.
- [11] P. Dagaut, A. Nicolle, *Combust. Flame* 140 (2005) 161–171.

- [12] P. Dagaut, G. Dayma, *J. Phys. Chem. A* 110 (2006) 6608–6616.
- [13] J.M. Zalc, W.H. Green, E. Iglesia, *Ind. Eng. Chem. Res.* 45 (2006) 2677–2688.
- [14] R. Sivaramakrishnan, K. Brezinsky, G. Dayma, P. Dagaut, *Phys. Chem. Chem. Phys.* 9 (2007) 4230–4244.
- [15] C.L. Rasmussen, A.E. Rasmussen, P. Glarborg, *Combust. Flame* 154 (2008) 529–545.
- [16] A. Doughty, F.J. Barnes, J.H. Bromly, B.S. Haynes, *Proc. Combust. Inst.* 26 (1996) 589–596.
- [17] P. Dagaut, O. Mathieu, A. Nicolle, G. Dayma, *Combust. Sci. Tech.* 177 (2005) 1767–1791.
- [18] J.G. Lopez, C.L. Rasmussen, M.U. Alzueta, Y. Gao, P. Marshall, P. Glarborg, *Proc. Combust. Inst.* 32 (2009) 367–375.
- [19] A.A. Konnov, F.J. Barnes, J.H. Bromly, J.N. Zhu, D.K. Zhang, *Combust. Flame* 141 (2005) 191–199.
- [20] M. Slack, A. Grillo, *Investigation of Hydrogen-Air Ignition Sensitized by Nitric Oxide and by Nitric Dioxide*, NASA Report No. 2896, NASA Washington, DC, 1977.
- [21] M.W. Slack, A.R. Grillo, *Combust. Flame* 31 (1978) 275–283.
- [22] S. Gersen, N.B. Anikin, A.V. Mokhov, H.B. Levinsky, *Int. J. Hydrogen Energy* 33 (2008) 1957–1964.
- [23] S. Gersen, A.V. Mokhov, J.H. Darneveil, H.B. Levinsky, *Combust. Flame* 157 (2010) 240–245.
- [24] C.L. Rasmussen, J. Hansen, P. Marshall, P. Glarborg, *Int. J. Chem. Kinet.* 40 (2008) 454–480.
- [25] C.L. Rasmussen, J.G. Jacobsen, P. Glarborg, *Int. J. Chem. Kinet.* 40 (2008) 778–807.
- [26] J. Gimenez, C.L. Rasmussen, M.U. Alzueta, P. Marshall, P. Glarborg, *Proc. Combust. Inst.* 32 (2009) 367–375.
- [27] J. Giménez-López, M.U. Alzueta, C.L. Rasmussen, P. Marshall, P. Glarborg, *Proc. Combust. Inst.* 33 (2011) 449–457.
- [28] E.L. Petersen, D.M. Kalitan, S. Simmons, G. Bourque, H.J. Curran, J.M. Simmie, *Proc. Combust. Inst.* 31 (2007) 447–454.
- [29] A.M. Dean, J.W. Bozzelli, *Combustion chemistry of nitrogen*, in: W.C. Gardiner (Ed.), *Gas Phase Combustion Chemistry*, Springer-Verlag, New York, 2000 (Chapter 2).
- [30] M.W. Slack, A.R. Grillo, *Proc. Int. Symp. Shock Tubes Waves* 11 (1978).
- [31] D. Lee, *Autoignition Measurements and Modelling in a Rapid Compression Machine*, Ph.D. Thesis, MIT, 1997.
- [32] G. Mittal, C.J. Sung, R.A. Yetter, *Int. J. Chem. Kinet.* 38 (2006) 516–529.
- [33] S. Tanaka, F. Ayala, J.C. Keck, *Combust. Flame* 133 (2003) 467–481.
- [34] G. Mittal, C.J. Sung, *Combust. Flame* 150 (2007) 355–368.
- [35] S.M. Gallagher, H.J. Curran, W.K. Metcalfe, D. Healy, J.M. Simmie, G. Bourque, *Combust. Flame* 153 (2008) 316–333.
- [36] A.E. Lutz, R.J. Kee, J.A. Miller, *SENKIN: A FORTRAN Program for Predicting Homogeneous Gas Phase Chemical Kinetics with Sensitivity Analysis*, Sandia Report SAND87-8248, Sandia National Laboratories, 1987.
- [37] J. Huang, W.K. Bushe, *Combust. Flame* 144 (2006) 74–88.
- [38] T. Faravelli, A. Frassoldati, E. Ranzi, *Combust. Flame* 132 (2003) 188–207.
- [39] P. Glarborg, *Proc. Combust. Inst.* 31 (2007) 77–98.
- [40] K. Glänzer, J. Troe, *Helv. Chim. Acta* 56 (1973) 577–585.
- [41] T.L. Cottrell, T.E. Graham, T.J. Reid, *Trans. Faraday Soc.* 47 (1951) 1088–1092.
- [42] K.A. Wilde, *Ind. Eng. Chem.* 48 (1956) 769–773.
- [43] K.A. Wilde, *J. Phys. Chem.* 61 (1957) 385–388.
- [44] V.V. Dubikhin, G.M. Nazin, G.B. Manelis, *Bull. Acad. Sci. USSR Div. Chem. Sci.* 7 (1971) 1412.
- [45] C. Canosa, R.-D. Penzhorn, C. von Sonntag, *Ber. Bunsenges. Phys. Chem.* 83 (1979) 217–225.